

MODIFIED LINEAR VISCOELASTIC MODEL OF EARTHQUAKE-INDUCED STRUCTURAL POUNDING*

S. MAHMOUD¹ AND R. JANKOWSKI^{2**}

¹Faculty of Eng. at Mataria, Helwan University, 11718 Cairo, Egypt

²Gdansk University of Technology, Faculty of Civil and Environmental Engineering,
ul. Narutowicza 11/12, 80-233 Gdansk, Poland
Email:jankowr@pg.gda.pl

Abstract– In recent times, earthquake-induced structural pounding has been intensively studied through the use of different impact force models. The numerical results obtained from the previous studies indicate that the linear viscoelastic model is relatively simple and accurate in modeling pounding-involved behavior of structures during earthquakes. The only shortcoming of the model is a negative value of the pounding force occurring just before separation, which has no physical explanation. The aim of the present paper is to verify the effectiveness of the modified linear viscoelastic model, in which the damping term is activated only during the approach period of collision, therefore overcoming this disadvantage. First, the analytical formula between the impact damping ratio and the coefficient of restitution is reassessed in order to satisfy the relation between the post-impact and the prior-impact relative velocities. Then, the performance of the model is checked in a number of comparative analyses, including numerical simulation of pounding-involved response, as well as comparison with the results of the impact experiment and shaking table experiments concerning pounding between two steel towers excited by harmonic waves. The final outcome of this study demonstrates that the results obtained through the modified linear viscoelastic model without the tension force are comparably similar to those found by using the linear viscoelastic model.

Keywords– Viscoelastic model, structural pounding, earthquakes, impact damping ratio, coefficient of restitution

1. INTRODUCTION

Interactions between adjacent buildings or bridge elements, known as structural pounding, have often been observed during earthquakes. The main reason of pounding is usually related to the difference in dynamic characteristics between adjacent structures [1, 2] and concerns, in particular, these structures, which induce relatively large drifts under earthquake excitation [3].

Structural pounding during earthquakes has recently been intensively studied using different models of collisions applied to different types of structures. The fundamental study on pounding between buildings in series, using the linear viscoelastic model of pounding force, was conducted by Anagnostopoulos [1]. Jankowski *et al.* [4] used the same model to study pounding of adjacent superstructure segments in elevated bridges. Other models of pounding force during impact, such as the linear elastic model [5, 6], the nonlinear elastic model [7, 8], the nonlinear viscoelastic model [9] and the Hertz-damp model [10], have also been implemented in the analyses.

It has been verified through the experiments [9] that the linear viscoelastic model is one of the most accurate among the above models. In this model, the pounding force F during impact is defined as [1]

*Received by the editors January 13, 2010; Accepted October 5, 2010.

**Corresponding author

$$F = k_k \delta + c_k \dot{\delta} \quad (1)$$

where δ , $\dot{\delta}$, k_k , and c_k denote the deformation of colliding structures with masses m_1 , m_2 , their relative velocity, the impact stiffness coefficient and the impact damping coefficient, which accounts for the energy dissipation during contact and which can be obtained from the formula [1]

$$c_k = 2\xi \sqrt{k_k \frac{m_1 m_2}{m_1 + m_2}} \quad (2)$$

where ξ is an impact damping ratio related to a well-known coefficient of restitution e by equation [11]

$$\xi = \frac{-\ln e}{\sqrt{\pi^2 + (\ln e)^2}} \quad (3)$$

Accounting for the energy dissipation during contact, which can result from plastic deformations, local cracking, friction, etc., makes the linear viscoelastic model very attractive in simulating more plastic impacts. Moreover, the model is relatively simple, and therefore can be easily applied in most of the computer codes. However, the linear viscoelastic model has a major shortcoming related to the negative impact force observed just before separation of colliding structures [9], which does not have any physical explanation [12,13]. This behavior results from the fact that the linear damping term in the model is activated during the whole time of contact (Eq. (1)) assuming a uniform dissipation of energy. Meanwhile, the results of experiments indicate that most of the energy is dissipated during the first phase of contact (approach period) and the second phase (restitution period) is mainly attributed to the elastic behavior where the accumulated elastic strain energy is released with minor energy loss due to friction [14].

In order to overcome the above drawback of the linear viscoelastic model, Valles and Reinhorn [15] proposed a variation of the model, in which the damping term is only active for positive velocities allowing the masses to release at time $t_{tot} = t_{max} + \frac{\pi}{2\omega_d}$, where $t_{max} = \frac{1}{\omega_d} \tan^{-1}(\frac{\omega_d}{\xi\omega_c})$ is the time of maximum deformation. Hence, the equivalent coefficient of restitution e can be described as $e = \sin(\omega_d t_{max}) \exp(-\xi\omega_c t_{max})$, where ω_d and ω_c is the damped and undamped circular frequency, respectively. However, no numerical analysis has been conducted to investigate the performance of the proposed model of pounding force during impact.

The aim of the present paper is to verify the effectiveness of the modified linear viscoelastic model, in which the damping term is activated only during the approach period of collision. First, the analytical formula between the impact damping ratio and the coefficient of restitution is reassessed in order to satisfy the relation between the post-impact and the prior-impact relative velocities. In order to verify the performance of the model, a number of numerical comparative analyses are conducted. The acceleration time history corresponding to the 1940 El Centro earthquake is first applied to two adjacent structures with an insufficient gap distance modeled as two single degree of freedom (SDOF) systems. The second and third numerical comparative analyses use the results of the impact experiment as well as the results of the shaking table experiments on pounding between two steel towers excited by harmonic wave.

2. ANALYTICAL RELATIONS

a) Force reformulation

The activation of the damping term during the whole time of collision results in a negative tensile force just before separation of the colliding structures. To overcome this disadvantage of the linear viscoelastic

model, the damping term is considered to be activated only during the approach period of collision, in which most of the energy is dissipated [14]. The pounding force F during impact in the modified linear viscoelastic model can be expressed as (compare Eq. (1))

$$\begin{aligned} F &= k_k \delta + c_k \dot{\delta} & \text{for } \dot{\delta} > 0 & \quad (\text{approach period of collision}) \\ F &= k_k \delta & \text{for } \dot{\delta} \leq 0 & \quad (\text{restitution period of collision}) \end{aligned} \quad (4)$$

b) Derivation of the relations between ξ and e

The relation between the impact damping ratio and the coefficient of restitution (3) is no longer valid due to the activation of the damping term in the approach period only. A reassessment of the relation between ξ and e , based on the reformulation of the pounding force (Eq. (4)), can be derived using a methodology based on the energy methods [14, 16] as follows:

Let v_i be the prior-impact (approaching) velocity of the colliding structure with mass m_i ($i=1,2$). The loss in kinetic energy after impact can be expressed in terms of the coefficient of restitution e and the relative prior-impact velocity $\dot{\delta}_0 = v_1 - v_2$ as [14]

$$\Delta E = \frac{1}{2} \frac{m_1 m_2}{m_1 + m_2} (1 - e^2) (\dot{\delta}_0)^2 \quad (5)$$

In the modified linear viscoelastic model, the dissipated energy by the damping term follows the relation

$$\Delta E = \int_0^{\delta_{\max}} c_k \dot{\delta} d\delta = 2\xi \sqrt{k_k \left(\frac{m_1 m_2}{m_1 + m_2} \right)} \int_0^{\delta_{\max}} \dot{\delta} d\delta \quad (6)$$

where $\dot{\delta}$ and δ_{\max} denote the relative velocity between the colliding structures during the approach period ($\dot{\delta} > 0$) and the maximum deformation, respectively.

An expression for the relative velocity $\dot{\delta}$ during the approach period, in terms of the deformation δ has to be obtained to evaluate the integral in Eq. (6). For simplicity, we first obtain a formula for the relative velocity $\dot{\delta}$ during the restitution period ($\dot{\delta} \leq 0$), which is considered to be the fully elastic period Eq. (4). Then, based on the assumed approximating functions, the relative velocity $\dot{\delta}$ during the approach period ($\dot{\delta} > 0$) can be obtained in terms of the deformation δ .

Equating the accumulated elastic strain energy at the beginning of the restitution period (i.e. at the point of maximum deformation δ_{\max}) with the kinetic energy at the time of separation yields

$$\int_0^{\delta_{\max}} F d\delta = \int_0^{\delta_{\max}} k_k \delta d\delta = \frac{1}{2} \frac{m_1 m_2}{m_1 + m_2} (\dot{\delta}_f)^2 \quad (7)$$

where $\dot{\delta}_f$ is the post-impact (final) relative velocity. Solving Eq. (7) for δ_{\max} yields

$$\delta_{\max} = \dot{\delta}_f \sqrt{\frac{m_1 m_2}{(m_1 + m_2) k_k}} \quad (8)$$

Due to the energy transfer from the elastic strain energy to kinetic energy, the following condition holds in the restitution period

$$\int_0^{\delta} k_k \delta d\delta + \frac{1}{2} \frac{m_1 m_2}{m_1 + m_2} (\dot{\delta})^2 = \frac{1}{2} \frac{m_1 m_2}{m_1 + m_2} (\dot{\delta}_f)^2 \quad (9)$$

Solving Eq. (9) allows us to determine the formula for the relative velocity $\dot{\delta}$ during the restitution period

($\dot{\delta} \leq 0$) as

$$\dot{\delta} = -\sqrt{(\dot{\delta}_f)^2 - k_k \left(\frac{m_1 + m_2}{m_1 m_2} \right) \delta^2} \quad (10)$$

Let us now consider two different approximating functions [17] to obtain two different expressions for the relative velocity $\dot{\delta}$ during the approach period of collision ($\dot{\delta} > 0$).

1. Expression 1: Taking into consideration Eq. (10) and assuming that the formula $e = \frac{|\dot{\delta}_f|}{\dot{\delta}_0}$, defining the relation between the post-impact and prior-impact relative velocities [14], is also valid for all values of deformation during the approach period of collision, the formula for the relative velocity $\dot{\delta}$ during the approach period ($\dot{\delta} > 0$) can be expressed as

$$\dot{\delta} = \frac{1}{e} \sqrt{(\dot{\delta}_f)^2 - k_k \left(\frac{m_1 + m_2}{m_1 m_2} \right) \delta^2} \quad (11)$$

After substituting Eq. (11) into Eq. (6) we obtain

$$\Delta E = 2 \frac{\xi}{e} \sqrt{k_k \left(\frac{m_1 m_2}{m_1 + m_2} \right)} \int_0^{\delta_{\max}} \sqrt{(\dot{\delta}_f)^2 - k_k \left(\frac{m_1 + m_2}{m_1 m_2} \right) \delta^2} d\delta \quad (12)$$

Substituting the formula for $\dot{\delta}_f$ obtained from Eq. (8) into Eq. (12) and simplifying the resulting expression leads to

$$\Delta E = 2 \frac{\xi k_k}{e} \int_0^{\delta_{\max}} \sqrt{\delta_{\max}^2 - \delta^2} d\delta \quad (13)$$

Integrating Eq. (13) leads to

$$\Delta E = \frac{\pi}{2} \frac{\xi k_k \delta_{\max}^2}{e} \quad (14)$$

Equating Eq. (14) and Eq. (5) yields

$$\frac{\pi}{2} \frac{\xi k_k \delta_{\max}^2}{e} = \frac{1}{2} \frac{m_1 m_2}{m_1 + m_2} (1 - e^2) (\dot{\delta}_0)^2 \quad (15)$$

Substituting Eq. (8) into Eq. (15) and solving for ξ gives

$$\xi = \frac{e(1 - e^2)}{\pi} \frac{(\dot{\delta}_0)^2}{(\dot{\delta}_f)^2} \quad (16)$$

Making use of the formula $e = \frac{|\dot{\delta}_f|}{\dot{\delta}_0}$ by substituting it into Eq. (16) allows us to describe the relation between the coefficient of restitution and the impact damping ratio for the modified linear viscoelastic model according to the formula

$$\xi = \frac{1}{\pi} \frac{1 - e^2}{e} \quad (17)$$

2. Expression 2: In the second approximation let us consider the formula for the relative velocity $\dot{\delta}$ during the approach period ($\dot{\delta} > 0$) as a sum of two expressions [17]. The first expression is identical to

Eq. (10), except for the sign change, whereas the second one increases the velocity in order to satisfy the relation $e = \frac{|\dot{\delta}_f|}{\dot{\delta}_0}$, assuming that the loss of difference of velocities $\dot{\delta}_0 - |\dot{\delta}_f|$ is uniform during the whole approach period. If so, then we can express the formula for the relative velocity $\dot{\delta}$ during the approach period ($\dot{\delta} > 0$) as

$$\dot{\delta} = \sqrt{(\dot{\delta}_f)^2 - k_k \left(\frac{m_1 + m_2}{m_1 m_2} \right) \delta^2} + \frac{(\dot{\delta}_0 - |\dot{\delta}_f|)(\delta_{\max} - \delta)}{\delta_{\max}} \quad (18)$$

Substituting Eq. (18) into Eq. (6) yields

$$\begin{aligned} \Delta E = & 2\xi \sqrt{k_k \left(\frac{m_1 m_2}{m_1 + m_2} \right)} \int_0^{\delta_{\max}} \sqrt{(\dot{\delta}_f)^2 - k_k \left(\frac{m_1 + m_2}{m_1 m_2} \right) \delta^2} d\delta \\ & + 2\xi \sqrt{k_k \left(\frac{m_1 m_2}{m_1 + m_2} \right)} \frac{(\dot{\delta}_0 - |\dot{\delta}_f|)(\delta_{\max} - \delta)}{\delta_{\max}} \int_0^{\delta_{\max}} (\delta_{\max} - \delta) d\delta \end{aligned} \quad (19)$$

Simplifying the above formula by making use of the derivation of Eq. (14) leads to

$$\Delta E = \frac{\pi}{2} \xi k_k \delta_{\max}^2 + 2\xi \sqrt{k_k \left(\frac{m_1 m_2}{m_1 + m_2} \right)} \frac{(\dot{\delta}_0 - |\dot{\delta}_f|)}{\delta_{\max}} \int_0^{\delta_{\max}} (\delta_{\max} - \delta) d\delta \quad (20)$$

Integrating the second term in Eq. (20) allows the equation to take the following form

$$\Delta E = \frac{\pi}{2} \xi k_k \delta_{\max}^2 + \xi \sqrt{k_k \left(\frac{m_1 m_2}{m_1 + m_2} \right)} (\dot{\delta}_0 - |\dot{\delta}_f|) \delta_{\max} \quad (21)$$

Equating Eq. (21) and Eq. (5) yields

$$\frac{1}{2} \frac{m_1 m_2}{m_1 + m_2} (1 - e^2) (\dot{\delta}_0)^2 = \frac{\pi}{2} \xi k_k \delta_{\max}^2 + \xi \sqrt{k_k \left(\frac{m_1 m_2}{m_1 + m_2} \right)} (\dot{\delta}_0 - |\dot{\delta}_f|) \delta_{\max} \quad (22)$$

Substituting Eq. (8) into Eq. (22) and solving for ξ relates the impact damping ratio as a function of the coefficient of restitution as

$$\xi = \frac{1 - e^2}{e(e(\pi - 2) + 2)} \quad (23)$$

The relations between the coefficient of restitution and the impact damping ratio for both the linear and modified linear viscoelastic models are shown in Fig. 1.

3. NUMERICAL STUDY

Using Eq. (23) we assess the performance of the modified linear viscoelastic model in capturing the earthquake-induced pounding compared with the linear viscoelastic model [1] and the nonlinear viscoelastic model [9], through three different procedures of comparison. The first one is based on simulation using the El Centro earthquake of 1940. Two single degree of freedom (SDOF) systems shown in Fig. 2, as models of two structures with equal masses and different natural periods, are used in the study. The second procedure is based on the impact experiment. The third uses the shaking table

experiments on pounding between two steel towers. The accuracy of each model in the second and the third procedure is assessed by calculating the normalized error NE to indicate the difference between the experimental and numerical results

$$NE = \frac{\|H - \bar{H}\|}{\|H\|} \cdot 100\% \quad (24)$$

where H is the response time history obtained experimentally, \bar{H} is the response time history obtained numerically, and $\|\cdot\|$ is the Euclidean norm. $\|H - \bar{H}\|$ and $\|H\|$, in the case of the time histories given in a discrete form, can be calculated as

$$\|H - \bar{H}\| = \sqrt{\sum_{i=1}^n (H_i - \bar{H}_i)^2}, \quad \|H\| = \sqrt{\sum_{i=1}^n H_i^2} \quad (25)$$

where n is a number of values in the time history record.

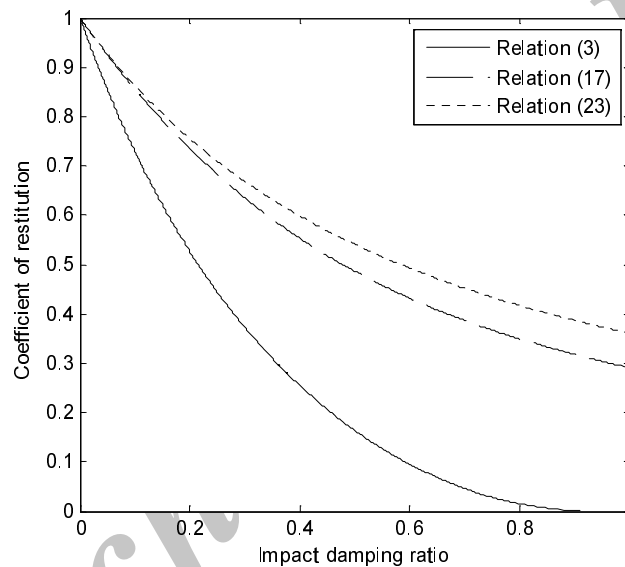


Fig. 1. Relations between the coefficient of restitution and damping ratio for the linear viscoelastic model and the modified linear viscoelastic model

a) Comparative analysis 1 – comparison based on numerical results

The El Centro earthquake of 1940 is applied to two SDOF models (Fig. 2), with the parameters described in [18], using three different pounding force models. The peak values of displacement, velocity, acceleration and pounding force for each model are obtained. For $i = 1, 2$ let m_i be the masses, c_i be the viscous damping coefficients, and k_i be the stiffness for SDOF 1 and SDOF 2, respectively. The coupling equation of motion for two adjacent structures subjected to horizontal ground motion \ddot{u}_g has the following form

$$\begin{aligned} m_1 \ddot{u}_1 + c_1 \dot{u}_1 + k_1 u_1 + F &= -m_1 \ddot{u}_g \\ m_2 \ddot{u}_2 + c_2 \dot{u}_2 + k_2 u_2 - F &= -m_2 \ddot{u}_g \end{aligned} \quad (26)$$

where u_i , \dot{u}_i and \ddot{u}_i represent the displacement, velocity and acceleration of the system, respectively, whereas F stands for the pounding force. The values of structural stiffness and damping coefficients: k_i , c_i can be calculated from the formulas [19]

$$k_i = \frac{4\pi^2 m_i}{T_i^2}; \quad c_i = 2\xi_i \sqrt{k_i m_i} \quad (27)$$

where T_i , ξ_i ($i = 1, 2$) denote the natural structural vibration period and structural damping ratio, respectively. We have solved the coupled equation of motion (26) for the El Centro earthquake record. The structural responses obtained for the three different pounding force models are shown in Figs. 3-5. The differences between the peak values of the responses for the linear viscoelastic model and its modified version have been calculated as equal to: 0.4-1.6% for the peak displacements, 0.1-0.8% for the peak velocities, 1.5-2.6% for the peak accelerations and 6.8% for the peak pounding forces. Larger differences have been observed between the results obtained for the modified linear viscoelastic model and the nonlinear viscoelastic model (compare Fig. 4 with Fig. 5).

b) Comparative analysis 2 - comparison based on impact experiment

Van Mier *et al.* [20] carried out an experiment on collisions between a prestressed concrete pile and a concrete striker for different contact surface geometries, striker mass and impact velocity values. The dynamic equation of motion for pounding between a striker of mass m_1 and a prestressed fixed pile can be written as (see free body diagram in Fig. 6)

$$m_1 \ddot{u}_1 + \frac{m_1 g}{l} u_1 + F = 0 \quad (28)$$

where u_1 , \ddot{u}_1 , l are the displacement, acceleration and length of the pendulum striker, respectively, F is the pounding force and g stands for the acceleration of gravity. The results from the numerical simulations as well as the results of two experimental tests for the impact of a spherical concrete pendulum striker of mass 570 kg (concrete strength 38.2 N/mm²) with an impact velocity 0.5 m/s [20] are shown in Fig. 7. The following impact stiffness parameters have been used in the numerical analysis: $k_k = 9.35 \times 10^7$ N/m for the linear viscoelastic model, $k_k = 9.29 \times 10^7$ N/m for the modified linear viscoelastic model and $k_k = 2.75 \times 10^9$ N/m^{3/2} for the nonlinear viscoelastic model [9]. These values have been found through an iterative procedure in order to keep the maximum pounding force in the numerical analysis equal to the maximum pounding force of the experiment (102.5 kN). For all models, the coefficient of restitution $e = 0.65$ has been used. It has been found that the normalized error is equal to 23.8% for the linear viscoelastic model, 32.6% for the modified linear viscoelastic model and 22.9% for the nonlinear viscoelastic model.

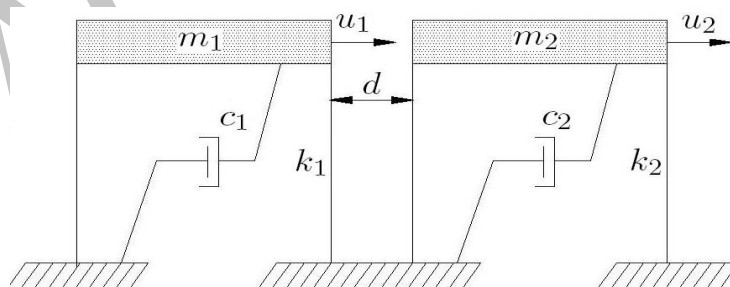


Fig. 2. Model idealization of adjacent structures

c) Comparative analysis 3 - comparison based on shaking table experiments

Chau *et al.* [21] carried out the shaking table tests to investigate the pounding phenomenon between two steel towers of different natural frequencies and damping ratios subjected to different combinations of stand-of distance and seismic excitations. Two single degree of freedom (SDOF) systems shown in Fig. 2, as models of two structures, are used in the numerical simulations. The dynamic equation of motion for

such a model is given by Eq. (26). We have solved the equation of motion (26) for the harmonic waves as excitations and three different models of pounding force considered herein. Chau *et al.* [21] performed a series of shaking table experiments for $n = 1$ (1 pounding per cycle) and $n = 2$ (1 pounding per 2 cycles) using various harmonic waves as excitations for two SDOF. Experimental, numerical and analytical results of the relative impact velocity versus the excitation frequency have been computed for the comparison purposes between experiments and theories.

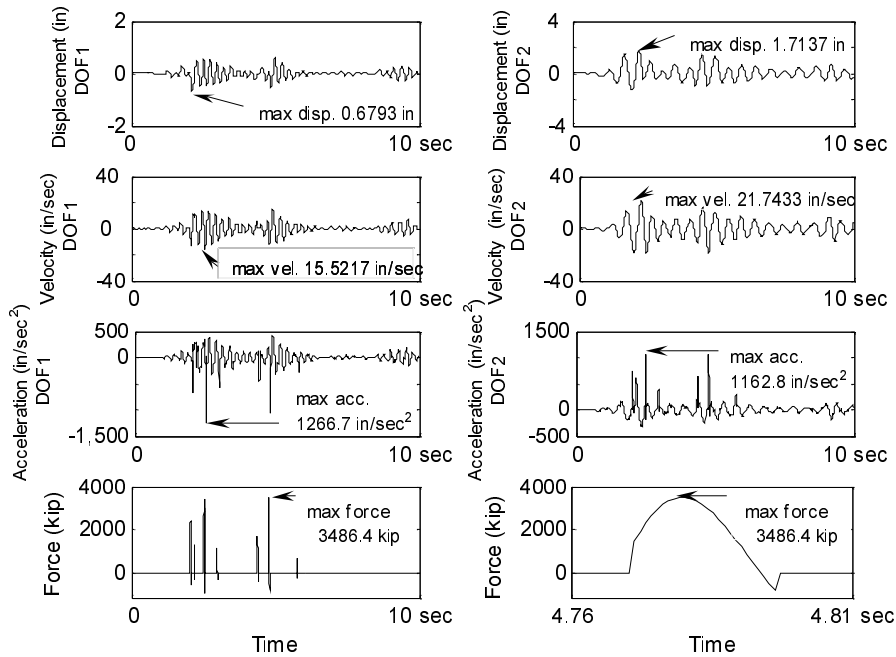


Fig. 3. Response of two SDOF building systems under the El Centro earthquake using the linear viscoelastic model

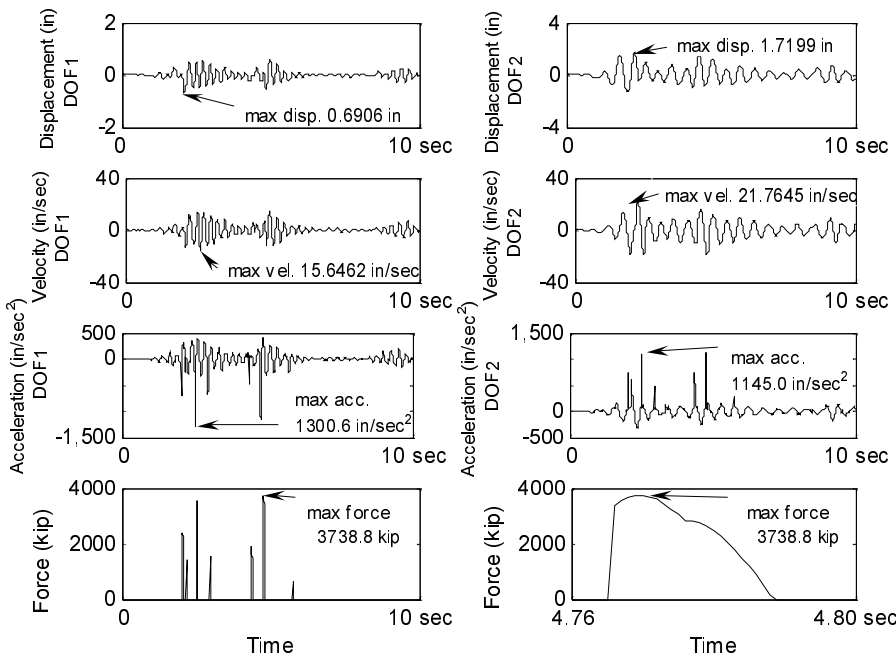


Fig. 4. Response of two SDOF building systems under the El Centro earthquake using the modified linear viscoelastic model

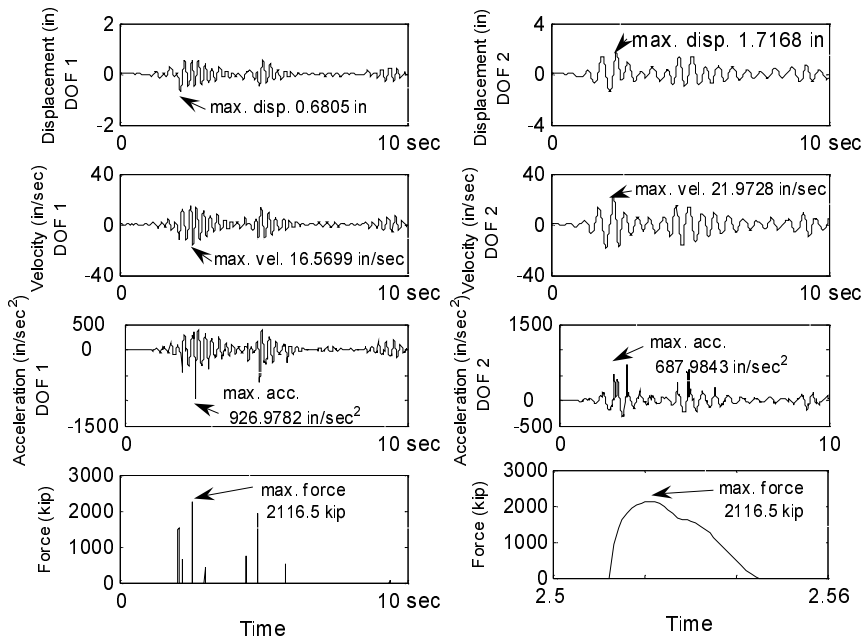


Fig. 5. Response of two SDOF building systems under the El Centro earthquake using the nonlinear viscoelastic model

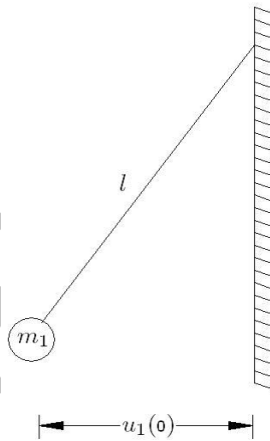


Fig. 6. Free body diagram for pounding between a concrete pendulum striker and prestressed concrete pile

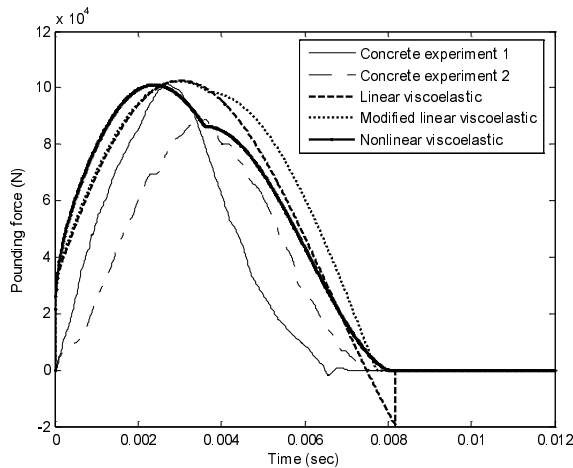


Fig. 7. Pounding force time histories during impact between a concrete pendulum striker and prestressed concrete pile

In this paper, the results of two different sinusoidal loads, as input excitations, are presented. First, we have considered the input shaking table of the form $\ddot{u}_g = 2.6 \sin(2\pi f_g t)$ as an excitation acting on SDOF 1 and SDOF 2 with the following dynamic characteristics: $m_1 = 98.0$ kg, $f_1 = 5.04$ Hz, $\xi_1 = 7.2\%$, $m_2 = 146.4$ kg, $f_2 = 2.76$ Hz, $\xi_2 = 1.5\%$ and a separation distance of 19.8 mm [21]. The numerical solutions for the steady state relative impact velocity using all three pounding force models have been compared with the experimental results [21] which are the average of 10 cycles in the steady state. The results from the numerical analysis and the experiment are shown in Fig. 8. The simulation errors for the numerically obtained impact velocity values compared with the experimental results for $n = 1$ and $n = 2$ are: 24.65% and 40.24% for the linear viscoelastic model, 26.78% and 43.19% for the modified linear viscoelastic model, 31.66% and 51.26% for the nonlinear viscoelastic model.

As a second input excitation, we have considered the harmonic excitation $\ddot{u}_g = 1.9 \sin(2\pi f_g t)$ applied to the SDOF 1 and SDOF 2 with the same dynamic characteristics and separation distance as used before. The results from the numerical analysis and the experiment are shown in Fig. 9. The simulation errors for the numerically obtained impact velocity values compared with the experimental results for $n = 1$ and $n = 2$ are: 27.64% and 69.08% for the linear viscoelastic model, 30.63% and 71.34% for the modified linear viscoelastic model, 33.75% and 59.80% for the nonlinear viscoelastic model.

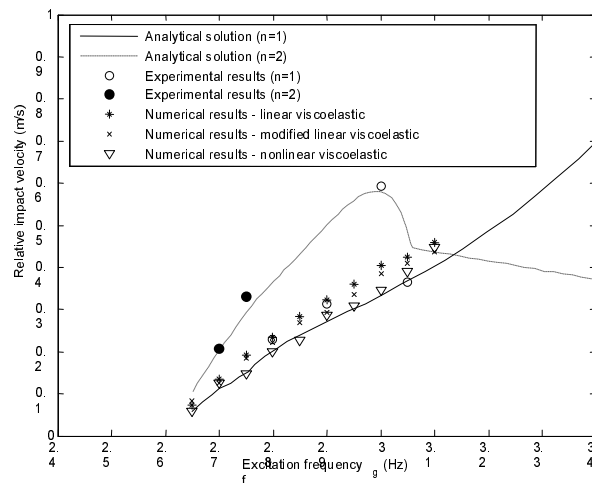


Fig. 8. The steady state relative impact velocity versus the excitation frequency under the input shaking table excitation $\ddot{u}_g = 2.6 \sin(2\pi f_g t)$

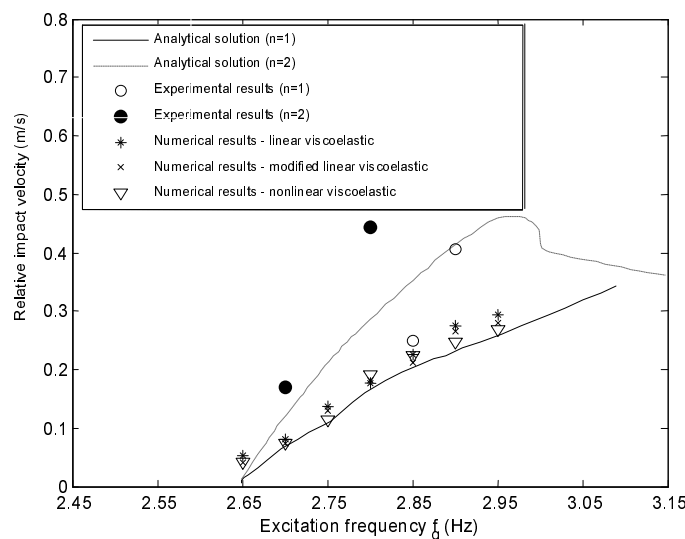


Fig. 9. The steady state relative impact velocity versus the excitation frequency under the input shaking table excitation $\ddot{u}_g = 1.9 \sin(2\pi f_g t)$

4. CONCLUSION

An improved version of the linear viscoelastic model of the earthquake-induced structural pounding, which overcomes the disadvantage of the tension force appearing just before separation between colliding structures, has been considered in this paper. In the modified linear viscoelastic model the minor energy loss during the restitution period is neglected and the damping term is activated only during the approach period of collision. Two analytical formulas relating the impact damping ratio and the coefficient of restitution have been derived based on the approximating functions. In order to verify the validity of the modified linear viscoelastic model, a number of comparative analyses have been carried out.

The results of the study presented in this paper indicate that the use of the modified linear viscoelastic model leads to very similar pounding-involved responses as in the case of the linear viscoelastic model. The comparison between the results of numerical simulations and experiments show that the linear viscoelastic model is more accurate than its modified version in all the cases considered. On the other hand, the modified linear viscoelastic model has been found to be more accurate than the nonlinear viscoelastic model in a few cases. Anyway, the results of the study indicate that the modification introduced in the linear viscoelastic model, in order to overcome the drawback which does not have a physical explanation, does not really lead to the improvement of the accuracy of the model. Therefore, the standard version of the linear viscoelastic model, being aware of its shortcoming, is recommended for the purposes of numerical simulations of the earthquake-induced structural pounding in future studies.

5. REMARK

The differential Eqs. (26) and (28) can be written in a uniform version

$$\begin{aligned} \frac{dp(u)}{dt} &= f(u), & t \geq 0 \\ u(0) &= u_0, \end{aligned} \quad (29)$$

where $u \in R^n$, $p : R^n \rightarrow R^n$ is a continuously differentiable function and $f : R^n \rightarrow R^n$ is a continuous function but not necessarily differentiable. Problem (29) is called a system of nonsmooth ordinary differential equations of the first order. In order to solve it efficiently we use the implicit Runge-Kutta (IRK) method [22-24] with various coefficients, such as coefficients of Gauss, Radau IA, Radau IIA, Lobatto IIIA, Burrage, etc. [22].

REFERENCES

1. Anagnostopoulos, S. A. (1988). Pounding of buildings in series during earthquakes. *Earthquake Engineering and Structural Dynamics*, Vol. 16, No. 3, pp. 443-456.
2. Ghafory-Ashtiany, M. (2001). The effect of random mass, stiffness and eccentricity parameters on seismic response of torsional system. *Iranian Journal of Science and Technology-Transaction B: Engineering*, Vol. 25, No. B1, pp. 93-114.
3. Aksogan, O., Murat Arslan, H. & Seren Akavci, S. (2003). Stiffened coupled shear walls on elastic foundation with flexible connections and stepwise changes in width, *Iranian Journal of Science and Technology, Transaction B: Engineering*, Vol. 27, No. B1, pp. 37-46.
4. Jankowski, R., Wilde, K. & Fujino, Y. Pounding of superstructure segments in isolated elevated bridge during earthquakes, *Earthquake Engineering and Structural Dynamics*, Vol. 27, No. 5, pp. 487-502.
5. Maison, B. F. & Kasai, K. (1990). Analysis for a type of structural pounding. *Journal of Structural Engineering (ASCE)*, Vol. 116, No. 4, pp. 957-977.

6. Maison, B. F. & Kasai, K. (1992). Dynamics of pounding when two buildings collide. *Earthquake Engineering and Structural Dynamics*, Vol. 21, No. 9, pp. 771-786.
7. Pantelides, C. P. & Ma, X. (1998). Linear and nonlinear pounding of structural systems. *Computers and Structures*, Vol. 66, No. 1, pp. 79-92.
8. Chau, K. T. & Wei, X. X. (2001). Pounding of structures modelled as non-linear impacts of two oscillators. *Earthquake Engineering and Structural Dynamics*, Vol. 30, No. 5, pp. 633-651.
9. Jankowski, R. (2005). Nonlinear viscoelastic modelling of earthquake-induced structural pounding. *Earthquake Engineering and Structural Dynamics*, Vol. 34, No. 6, pp. 595-611.
10. Muthukumar, S. & DesRoches, R. (2006). A Hertz contact model with nonlinear damping for pounding simulation. *Earthquake Engineering and Structural Dynamics*, Vol. 35, No. 7, pp. 811-828.
11. Anagnostopoulos, S. A. (2004). Equivalent viscous damping for modeling inelastic impacts in earthquake pounding problems. *Earthquake Engineering and Structural Dynamics*, Vol. 33, No. 8, pp. 897-902.
12. Hunt, K. H. & Crossley, F. R. E. (1975). Coefficient of restitution interpreted as damping in vibroimpact. *Journal of Applied Mechanics ASME*, Vol. 42, pp. 440-445.
13. Marhefka, D. W. & Orin, D. E. (1999). A compliant contact model with nonlinear damping for simulation of robotic systems. *IEEE Transactions on systems, Man, and Cybernetics- Part A: System and Humans*, Vol. 29, No. 6, pp. 566-572.
14. Goldsmith, W. (1960). *Impact: the theory and physical behaviour of colliding solids*. Edward Arnold, London.
15. Valles, R. E. & Reinhorn, A. M. (1996). Evaluation, prevention, and mitigation of pounding effects in building structures. *Proc. of the 11th World Conference on Earthquake Engineering*, Acapulco, Mexico, Paper No. 26.
16. Sheidaii, M. R., Abedi, K., Behraves, A. & Parke, G. A. R. (2003). An investigation into the collapse behaviour of double-layer space trusses. *Iranian Journal of Science and Technology, Transaction B: Engineering*, Vol. 27, No. B1, pp. 7-20.
17. Jankowski, R. (2006). Analytical expression between the impact damping ratio and the coefficient of restitution in the non-linear viscoelastic model of structural pounding. *Earthquake Engineering and Structural Dynamics*, Vol. 35, No. 4, pp. 517-524.
18. Muthukumar, S. & DesRoches, R. (2004). Evaluation of impact models for seismic pounding. *Proc. of the 13th World Conference on Earthquake Engineering*, Vancouver, Canada, Paper No. 235.
19. Harris, C. M. & Piersol, A. G. (2002). *Harris' shock and vibration handbook*. McGraw-Hill, New York.
20. Van Mier, J. G. M., Puijssers, A. F., Reinhardt, H. W. & Monnier, T. (1991). Load time response of colliding concrete bodies. *Journal of Structural Engineering (ASCE)*, Vol. 117, No. 2, pp. 354-374.
21. Chau, K. T., Wei, X. X., Guo, X. & Shen, C. Y. (2003). Experimental and theoretical simulation of seismic poundings between two adjacent structures. *Earthquake Engineering and Structural Dynamics*, Vol. 32, No. 4, pp. 537-554.
22. Jay, L. O. (2000). Inexact simplified Newton iterations for implicit Runge-Kutta methods. *SIAM Journal on Numerical Analysis*, Vol. 38, No. 4, pp. 1369-1388.
23. Chen, X. & Mahmoud, S. (2008). Implicit Runge-Kutta methods for Lipschitz continuous ordinary differential equations. *SIAM Journal on Numerical Analysis*, Vol. 46, No. 3, pp. 1266-1280.
24. Mahmoud, S. & Chen, X. (2008). A verified inexact implicit Runge-Kutta method for nonsmooth ODEs. *Numerical Algorithms*, Vol. 47, No. 3, pp. 275-290.